Random allocation models in the thermodynamic limit

Random allocation models in the thermodynamic limit

Piotr Bialas [*]
Institute of Applied Computer Science, Jagiellonian University, Ulica Lojasiewicza 11, 30-348 Kraków, Poland

Zdzislaw Burda [†]
Faculty of Physics and Applied Computer Science, AGH University of Krakow, Aleja Mickiewicza 30, 30-059 Kraków, Poland

Desmond A. Johnston [‡]
School of Mathematical and Computer Sciences, Heriot-Watt University, Riccarton, Edinburgh EH14 4AS, United Kingdom

(Received 1 August 2023; accepted 6 November 2023; published 5 December 2023)

We discuss the phase transition and critical exponents in the random allocation model (urn model) for different statistical ensembles. We provide a unified presentation of the statistical properties of the model in the thermodynamic limit, uncover relationships between the thermodynamic potentials, and fill some lacunae in previous results on the singularities of these potentials at the critical point and behavior in the thermodynamic limit. The presentation is intended to be self-contained, so we carefully derive all formulas step by step throughout. Additionally, we comment on a quasiprobabilistic normalization of configuration weights, which was considered in some recent studies.

DOI: 10.1103/PhysRevE.108.064107

I. INTRODUCTION

The random allocation model, also known as the balls-in-boxes model, the urn model, or the backgammon model [1–3], is a simple statistical model describing weighted random partitions of particles between boxes. Despite its simplicity, the model exhibits very rich critical behavior, including discontinuous and continuous phase transitions of different orders depending on the model parameters and the ensemble being considered. The phase transition in the model is related to a real-space condensation observed in many statistical problems including zero-range processes [4–11], mass transport [12–14], random trees [15,16], and quantum gravity [3,17,18]. The model has been used to understand some aspects of nonequilibrium dynamics of condensate formation [8]. The balls-in-boxes model has also been applied in studies of such diverse problems as wealth condensation [19] and the diversity of Zipf's populations [20]. The model can be used to mimic phase separation [21,22], condensation in complex networks [23,24], fireball formation at the Van Hove singularity [25], formation of a giant component or cluster in networks or percolation models, and the statistics of the longest interval in tied-down renewal processes [26–28]. The latter phenomenon is closely related to the appearance of big jumps in random walks with subexponentially distributed jump sizes, as described in [29].

In the present paper we revisit the issue of the phase transition in the model and analyze it carefully from the point of view of equilibrium statistical mechanics. We describe in detail how the order of the transition depends on the parameters of the model in various ensembles and present some results on the singularities of the thermodynamic potentials and the relationships between them. We also revisit the issue of finite-size effects by illustrating a typical evolution of the particle distribution with the increasing system size in the condensed phase, which reveals a nonuniform convergence to the limiting distribution. We discuss the interpretation of the deviations of the particle distribution for finite systems from the limiting distribution in light of various rigorous results on the nature of the condensate in [8,30–36]. Related work on the nature of the condensate in mass transport models and finite-size corrections may be found in [12,13]. In addition, we discuss some subtleties in a quasiprobabilistic normalization used in [20,32], which regularizes an otherwise divergent sum over the weights, and elucidate its exact relation to the class of models here.

The paper is organized as follows. In Sec. II we introduce a canonical ensemble and the basic quantities that describe the behavior of the system in this canonical ensemble. In Sec. III we apply the saddle-point method to calculate the free-energy density of the system in the canonical ensemble for low particle densities that are smaller than some critical density ρ_c in a thermodynamic limit in which the numbers of particles S and boxes N are sent to infinity at some fixed density. A detailed saddle-point calculation of the particle distribution can be found in Appendix A. For densities larger than ρ_c the system exhibits a real-space condensation. In Sec. IV we note that whether there is a phase transition at a finite

[*]piotr.bialas@uj.edu.pl
[†]zdzislaw.burda@agh.edu.pl
[‡]D.A.Johnston@hw.ac.uk

critical density or not depends on the asymptotic behavior of the weights governing the particle distribution. This divides the weight functions into three families for which the system has only the fluid phase, only the condensed phase, or both phases with a phase transition between them at a finite critical density. In Sec. V we focus on power-law weights of the form $w(s) = s^{-\beta}$ for s particles in a box to analyze the types of possible phase transitions. The asymptotic properties of the polylogarithm, which is the generating function for power-law weights, are recalled in Appendix B. These are then applied in detailed calculations in Appendix C, where we derive the possible scenarios that depend on the power in the weight function and determine the free energy and its behavior at the critical point by evaluating the asymptotic behavior of the cumulant generating function of the weights. We find that the phase transition is second order for $\beta \in (3, +\infty)$. For $\beta = 3$ the phase transition is also second order but with a logarithmic discontinuity; for $\beta < 3$ the order of the transition increases as β approaches 2, eventually disappearing at $\beta = 2$.

In Sec. VI we repeat these steps for a grand-canonical ensemble in which the number of boxes is allowed to fluctuate while taking the thermodynamic limit. This reveals that, while the canonical system has a continuous phase transition of arbitrary order as β is varied, the grand-canonical system may additionally display a discontinuous (i.e., first-order) phase transition. The details of these calculations may be found in Appendix D, where we employ asymptotic methods similar to those used in investigating the canonical ensemble to show that the phase transition in the grand-canonical ensemble is first order for $\beta \in (2, +\infty)$ and that for $\beta \in (1, 2]$ the order of the phase transition varies from second to infinite. It should be noted that the term "grand-canonical" is usually used to refer to statistical systems with a fluctuating number of particles, while here we apply it to a system with a fluctuating number of boxes, which plays the role of the volume of the system.

The standard grand-canonical ensemble with a fluctuating number of particles is discussed in Sec. VII. As we will see, in this case the partition function entirely factorizes so the system is in a sense trivial. An ensemble with a varying number of both particles and boxes is also defined. We move on in Sec. VIII to discuss ensembles with the quasiprobabilistic weights of [20,32] and their relation to the other ensembles discussed here. We conclude with a short summary in Sec. IX, which reiterates the main results on the phase structure in the canonical and grand-canonical ensembles and emphasizes the Legendre-Fenchel transform relationship between the thermodynamic potentials in the two ensembles. We also note that the grand-canonical potential is just the inverse function of the cumulant generating function of the weights. Finally, we advertise further work using the methods deployed in this paper to evaluate Rényi entropies for zeta urns and to calculate the partition function zeros of the model.

II. CANONICAL ENSEMBLE

The balls-in-boxes model is defined by the partition function [1]

$$Z_{S,N} = \sum_{(s_1,\ldots,s_N)} w(s_1)\cdots w(s_N)\delta_{S-(s_1+\cdots+s_N)} \tag{1}$$

that describes weighted distributions of S particles in N boxes, where the s_i denote the occupations of boxes $i = 1, \ldots, N$. The lowercase δ represents the Kronecker delta: $\delta_n = 1$ for $n = 0$ and $\delta_n = 0$ for all other integers $n \neq 0$. The δ in Eq. (1) selects configurations that have exactly S particles in N boxes. The statistical weight of a configuration $(s_1, s_2, \ldots, s_N)$, which describes the partition of particles between boxes, is the product of statistical weights $w(s_i)$ of individual boxes, which depend only on the number of particles in the box. The numbers of particles in different boxes are almost independent of each other, but the constraint $s_1 + \cdots + s_N = S$ makes them weakly dependent. In some conditions, the presence of this constraint leads to a phase transition, as will be seen later.

In general, the statistical weight $s \to w(s)$ is a nonnegative real-valued function defined for $s = 0, 1, 2, \ldots$. However, we find it convenient to limit the range of s to positive integers $s = 1, 2, \ldots$, in which case each box must contain at least one particle and there must be at least $S = N$ particles in a system with N boxes. The full range (including empty boxes) can be always recovered by introducing new weights $w'(s) = w(s + 1)$ for $s = 0, 1, 2, \ldots$ and redefining the box occupation numbers $s'_i = s_i - 1$ and $S' = S - N$. In the following we assume that there are no empty boxes. This version of the model occurs naturally in many of the problems mentioned in the Introduction.

Let us consider a system with q balls in the first box. Then the rest of the boxes contain $S - q$ balls and are described by the partition function $Z_{S-q,N-1}$. This leads to the recurrence relation

$$Z_{S,N} = \sum_{q=1}^{S-N+1} w(q) Z_{S-q,N-1} \tag{2}$$

for $S \geqslant N \geqslant 1$ and

$$Z_{S,0} = \delta_S \tag{3}$$

for $N = 0$. The formula for $Z_{S,0}$ ensures that

$$Z_{S,1} = w(S),$$

as required.

Consider a physical quantity $O = O(s_1, \ldots, s_N)$. The ensemble average is defined as

$$\langle O\rangle_{S,N} = \frac{1}{Z_{S,N}} \sum_{(s_1,\ldots,s_N)} O(s_1, \ldots, s_N) \times w(s_1)\cdots w(s_N)\delta_{S-(s_1+\cdots+s_N)}. \tag{4}$$

It is worth noting that the transformation

$$w(s) \to e^{\lambda+\sigma s} w(s) \tag{5}$$

leaves the ensemble averages (4) unchanged,

$$\langle O\rangle_{S,N} \to \langle O\rangle_{S,N}, \tag{6}$$

because it introduces the same factors $e^{\lambda N+\sigma S}$ in the numerator and denominator of (4) and they cancel out. We will use this invariance in the following many times.

As an example, consider the fraction of sites with q particles in a given configuration $(s_1, s_2, \ldots, s_N)$:

$$\pi(q) = \frac{1}{N}\sum_{i=1}^{N} \delta_{q-s_i}. \tag{7}$$

The ensemble average of $\pi(q)$ can be calculated directly from the partition function by observing that if a box contains q particles then the remaining $N-1$ boxes contain $S-q$ particles. This leads to the relation

$$\langle \pi(q) \rangle_{S,N} = \frac{w(q) Z_{S-q,N-1}}{Z_{S,N}} \tag{8}$$

for $S \geqslant N \geqslant 1$ and $q = 1, 2, \ldots, S-N+1$. The relation (2) ensures that this distribution is normalized,

$$\sum_{q=1}^{S-N+1} \langle \pi(q) \rangle_{S,N} = 1. \tag{9}$$

As an illustration consider the model with weights $w(s) = 1$ for $s = 1, 2, \ldots$. One finds that

$$Z_{S,N} = \binom{S-1}{N-1} \tag{10}$$

and

$$\langle \pi(q) \rangle_{S,N} = \frac{\binom{S-1-q}{N-2}}{\binom{S-1}{N-1}} \tag{11}$$

for $q = 1, 2, \ldots$. Note that the invariance of the ensemble averages (6) under the transformation (5) leads to the somewhat counterintuitive conclusion that exponentially increasing or decreasing weights $w(s) = e^{\lambda+\sigma s}$ give exactly the same results as the constant weights $w(s) = 1$. In particular, the particle distribution for the exponentially increasing or decreasing weights will be given by (11). This is directly related to the well-known probabilistic fact that exponential random variables, conditioned on their sum, are uniformly distributed.

III. THERMODYNAMIC LIMIT

We are interested in the behavior of the system in the thermodynamic limit

$$S \to \infty, \quad \frac{N}{S} \to r, \tag{12}$$

where $r \in (0, 1)$. The behavior depends on the form of $w(s)$ but also on r, which is a free parameter of the model, being the reciprocal of the average particle density ρ:

$$\rho \equiv \frac{S}{N} = \frac{1}{r}. \tag{13}$$

We will use r and ρ interchangeably.

To describe the behavior of the system in the thermodynamic limit (12), it is convenient to introduce a thermodynamic potential

$$\phi(r) = \lim \frac{1}{S} \ln Z_{S,N}, \tag{14}$$

where lim in this equation means the limit (12). With a mild misuse of terminology, $\phi(r)$ may be called the free-energy density (free energy per particle). The free-energy density $\phi(r)$ is the rate of asymptotic growth of the partition function with the system size for given r,

$$Z_{S,N} \propto e^{S\phi(r)}, \tag{15}$$

in the thermodynamic limit (12). The subexponential corrections are omitted. For trivial weights, that is, for $w(s) = 1$ for $s = 1, 2, \ldots$, discussed in the preceding section, the partition function (10) behaves in this limit asymptotically as

$$Z_{S,N} \propto \frac{1}{\sqrt{2\pi S r(1-r)}} e^{-S[r \ln r + (1-r)\ln(1-r)]}, \tag{16}$$

so the free-energy density is

$$\phi(r) = -r \ln r - (1-r)\ln(1-r). \tag{17}$$

This can be seen by applying Stirling's formula to (10). It is also easy to see that the particle distribution (11) takes the asymptotic form in the limit (12),

$$\langle \pi(q) \rangle_{S,N} \propto \frac{r}{1-r} e^{-q \ln[1/(1-r)]}, \tag{18}$$

for $q = 1, 2, \ldots$. The asymptotic expressions (16) and (18) hold for any $r \in (0, 1)$. They break down for $r = 0$ (infinite density), that is, when the number of particles S grows faster than linearly with the number of boxes N as N goes to infinity. They also break down for $r = 1$, that is, when the difference $S - N$ grows slower than linearly with N as N goes to infinity.

In the general case, the thermodynamic potential $\phi(r)$ can be calculated using the saddle-point method. Using an integral representation of the Kronecker δ,

$$\delta_n = \int_{-\pi}^{\pi} \frac{d\alpha}{2\pi} e^{in\alpha}, \tag{19}$$

we can rewrite the partition function (1) as

$$Z_{S,N} = \int_{-\pi}^{\pi} \frac{d\alpha}{2\pi} e^{iS\alpha} \left(\sum_{s=1}^{\infty} w(s) e^{-is\alpha} \right)^N. \tag{20}$$

The right-hand side of this equation can be more concisely written as

$$Z_{S,N} = \int_{-\pi i}^{\pi i} \frac{d\alpha}{2\pi i} e^{S\alpha + NK(\alpha)}, \tag{21}$$

where $K(\alpha)$ is a cumulant generating function

$$K(\alpha) = \ln \sum_{s=1}^{\infty} w(s) e^{-s\alpha}. \tag{22}$$

In the limit (12), the leading contribution to the integral is

$$Z_{S,N} \propto e^{S\phi(r)}, \tag{23}$$

where

$$\phi(r) = \alpha(r) + rK(\alpha(r)), \tag{24}$$

with $\alpha(r)$ a solution of the saddle-point equation

$$\frac{1}{r} = -K'(\alpha(r)). \tag{25}$$

This result is obtained by deforming the integration contour so that it passes through a saddle point. The saddle point is located on the real axis and its position $\alpha(r)$ depends on the particle density. When the particle density $\rho = 1/r$ increases,

$\alpha(r)$ decreases. The minimal value that it may take is limited by $\alpha_c = -\ln R_c$, where

$$R_c = \limsup_{s\to\infty} \frac{1}{w(s)^{1/s}} \tag{26}$$

is the radius of convergence of the series (22). For the monotonic weights that we consider here

$$\alpha_c = \lim_{s\to\infty} \frac{\ln w(s)}{s}. \tag{27}$$

For $\alpha > \alpha_c$ the series in (22) is convergent. The saddle-point solution $\alpha(r)$ holds only for $r > r_c$,

$$r_c = -\frac{1}{K'(\alpha_c)}. \tag{28}$$

For $r \to r_c^+$, the saddle point $\alpha(r) \to \alpha_c$ approaches the singularity of $K(\alpha)$ (22).

In the thermodynamic limit (12), one can also derive (see Appendix A) an asymptotic form of the particle distribution (8),

$$\langle \pi(q)\rangle_{S,N} \propto \frac{w(q)e^{-q\alpha(r)}}{e^{K(\alpha(r))}} = \frac{w(q)e^{-q\alpha(r)}}{\sum_{s=1}^{\infty} w(s)e^{-s\alpha(r)}}. \tag{29}$$

We see that the distribution is suppressed by an exponential factor of approximately $\exp\{-q[\alpha(r) - \alpha_c]\}$ for large q.

The first moment of the particle distribution should be exactly equal to the particle density

$$\frac{1}{r} = \langle q\rangle_{S,N} \equiv \sum_{q=1}^{\infty} q\langle \pi(q)\rangle_{S,N}. \tag{30}$$

Replacing $\langle \pi(q)\rangle_{S,N}$ on the right-hand side of this equation with (29), we find

$$\frac{1}{r} = \frac{\sum_{q=1}^{\infty} qw(q)e^{-q\alpha(r)}}{\sum_{s=1}^{\infty} w(s)e^{-s\alpha(r)}} = -K'(\alpha(r)), \tag{31}$$

consistently with the saddle-point equation (25).

Above ρ_c another condensed phase appears: the condensed phase where an extensive (proportional to S) number of particles condense in one box. This was first observed in [1] and then rigorously proven in [30–35]. In the next section we discuss in detail the phase transition between the two phases.

IV. PHASE STRUCTURE

As mentioned, the system can have two distinct phases: the fluid phase for small particle densities and the condensed phase for large particle densities. The fluid phase is described by the solution of the saddle-point equations (25) which correspond to a local solution of the maximization problem within the interval $(r_c, 1)$. In the condensed phase, the equations are no longer valid. In this case the maximal contribution to the free energy comes from the boundary at r_c. The critical density at which the transition from one phase to another occurs is given by $\rho_c = 1/r_c$, with r_c defined by (28). Whether the system has a phase transition or not depends on the weight function $w(s)$. Let us discuss the possible scenarios.

The set of possible weight functions can be divided into three families which are classified by the value of the parameter α_c (27): The first family includes weight functions $w(s)$ for which $\alpha_c = -\infty$, the second includes weights for which $\alpha_c = +\infty$, and the third includes weights for which α_c is a finite number.

(i) Weight functions $w(s)$ from the first family ($\alpha_c = -\infty$) fall off asymptotically to zero faster than exponentially for $s \to \infty$, for instance, $w(s) = 1/s!$ or $w(s) = e^{-s^2}$. Weights which vanish for all s above a certain value s_0, i.e., $w(s) = 0$ for all $s > s_0$, also belong to this category.

(ii) Weight functions $w(s)$ from the second family ($\alpha_c = +\infty$) grow faster than exponentially for $s \to \infty$, for instance, $w(s) = s!$ or $w(s) = e^{s^2}$.

(iii) Weight functions $w(s)$ from the third family ($-\infty < \alpha_c < +\infty$) neither increase nor decrease faster than exponentially for $s \to \infty$, for instance, $w(s) = e^{\sigma s}s^{-\beta}$ or $w(s) = e^{\pm\sqrt{s}}$. One should note that powerlike weights, $w(s) = s^{-\beta}$, belong to this category, even if β is negative.

For the first family the system has only the fluid phase, for the second one it has only the condensed phase. The third family, in a way, interpolates between the first two cases and therefore it is the most interesting one.

From now on, we focus on weight functions from the third family, such that α_c (27) is finite. Using the transformation (5), which does not affect the ensemble averages, we can transform the weights $w(s) \to e^{-\alpha_c s}w(s)$ so that the critical value (27) after the transformation is $\alpha_c = 0$. So from now on, unless we specify otherwise, we set by default $\alpha_c = 0$.

The inverse particle density r is a free parameter that can change in the range $r \in (0, 1)$. The saddle-point equation (25) holds for $r \in (r_c, 1)$, where r_c is given by (28) (with $\alpha_c = 0$). Two situations can be distinguished: $-K'(0)$ is infinite or finite. In the former case the critical density is infinite, so there is no phase transition and the saddle-point solution holds for the whole range of $r \in (0, 1)$. In the latter case, the critical density is finite, so there is a phase transition at $\rho_c = -K'(0)$. The saddle-point solution holds for $r \in (r_c, 1)$. As mentioned, in this case the particle distribution (29) falls off exponentially for large q as $\pi(q) \propto w(q)e^{-q\alpha(r)}$, with $\alpha(r) > 0$. At $r = r_c$ the exponential factor disappears, $\alpha(r_c) = 0$, and the particle distribution (29) tends in the thermodynamic limit (12) to its critical form

$$\langle \pi(q)\rangle_{S,N} \to \pi_c(q) \equiv \frac{w(q)}{K(0)} = \frac{w(q)}{\sum_{s=1}^{\infty} w(s)} \tag{32}$$

whose mean is equal to the critical density

$$\sum_{q=1}^{\infty} q\pi_c(q) = -K'(0) = \rho_c. \tag{33}$$

To see what happens for $\rho > \rho_c$, in the condensed phase, we perform a finite-size analysis. More precisely, we will numerically determine the particle distribution $\langle \pi(q)\rangle_{S,N}$ for finite N using the formula (8) and the recursion (2). In fact, instead of (2) we have used the recursion

$$Z_{S,2N} = \sum_{q=N}^{S-N} Z_{q,N}Z_{S-q,N} \tag{34}$$

in the calculations. It is more efficient than (2), because it doubles N in one step while (2) increases N by one.

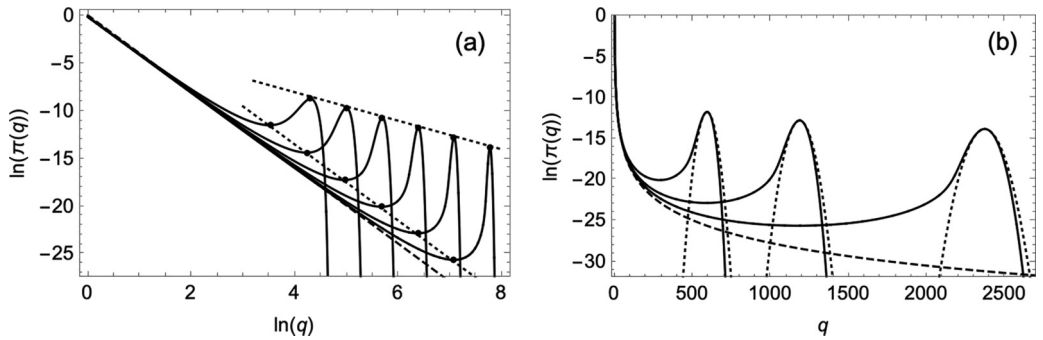

FIG. 1. Distribution $\langle \pi(q) \rangle_{S,N}$ for $N = 2^k + 1$, $\beta = 4$, and $S = \lceil 1.4N \rceil$. (a) Plot of the distribution for $k = 8, 9, \ldots 13$ in logarithmic scale. The dashed line represents the critical distribution $\pi_c(q) = q^{-4}/\zeta(4)$. The dotted lines pass through the local maxima and minima of the graphs. The heights of the maxima scale as $N^{-3/2}$ (38) and of the minima as N^{-4} [8]. (b) Plot of the distribution for $k = 11, 12, 13$ in semilogarithmic scale. As before, the dashed line (now a curve) represents the critical distribution. The dotted lines represent Gaussian curves with $S - (N-1)K'(0)$ means, $(N-1)K''(0)$ variances, and $1/N$ normalization.

As an example, we study the behavior of the system for power-law weights

$$w(s) = s^{-\beta}, \tag{35}$$

with $\beta = 4.0$ and $\rho = 1.4$, which is greater than the critical density

$$\rho_c = \frac{\zeta(3)}{\zeta(4)} \approx 1.11, \tag{36}$$

so the system is in the condensed phase. The results are presented in Fig. 1. As we can see from Fig. 1(a), the distribution can be divided into a bulk part corresponding to the critical distribution

$$\pi_c(q) = \frac{q^{-4}}{\zeta(4)}, \tag{37}$$

denoted by the dashed line in the figure and a peak. The peak is located at $Q \approx N(\rho - \rho_c)$. The area under the peak tends to $1/N$. This can be clearly seen in Fig. 1(b), where the peaks are compared to Gaussian curves with area $1/N$. This picture can be understood as a split of the system into a critical subsystem consisting of $N-1$ boxes and a single box that captures the excess particles that did not fit in the critical subsystem. This picture was conjectured in [1] and then rigorously proven (see, for instance, [8,30–36]).

The critical part consists of S_{N-1} particles in $N-1$ boxes. The S_{N-1} can be approximated as a sum of $N-1$ independent random numbers $q_1 + \cdots + q_{N-1}$ distributed according to the critical distribution $\pi_c(q)$. By the generalized central-limit theorem [37], such a sum grows on average as $(N-1)\rho_c$ and behaves in the limit $N \to \infty$ like a normal random variable with the variance $(N-1)K''(0)$ if $K''(0) < \infty$ or as a one-sided α-stable random variable with $\alpha \in (1,2)$ otherwise. This tells us that the number of particles in the remaining box is on average $Q = S - S_{N-1} \approx N(\rho - \rho_c)$, and its fluctuations about the mean are of order $\sqrt{N}$ if $K''(0) < \infty$ or $N^{1/\alpha}$ otherwise.

In the discussed example $K''(0) < \infty$, so the peak can be approximated by a normalized Gaussian curve with mean Q and variance $NK''(0)$,

$$\frac{1}{N}\pi_{\rm cond}(q) \approx \frac{1}{N}\frac{1}{\sqrt{2\pi N K''(0)}} \exp\left(-\frac{(q-Q)^2}{2NK''(0)}\right), \tag{38}$$

with an additional $1/N$ factor that reflects the fact that the condensate is in one of the N boxes. The height of the peak is of order $N^{-3/2}$, as follows from (38).

The approach to the limit distribution (37) is very slow and nonuniform, as shown in Fig. 1. The peak which is present for any finite N does not disappear but moves away to infinity when N increases. The shape of the peak deviates from the Gauss-curve shape. The deviations are seen as long tails on the left side of parabolas in a semilogarithmic plot. Slight deviations of tails on the right-hand side can also been seen. The left tails are remnants of the power-law tail $q^{-\beta}$ of the critical distribution (32) [8]. The contribution from the tails decreases as N grows, as discussed below. The excess probability accumulated in the left tails,

$$P_{\rm dev} = \sum_{q=1}^{q_{\max}} \left(\langle \pi(q) \rangle_{S,N} - \frac{N-1}{N}\pi_c(q) - \frac{1}{N}\pi_{\rm cond}(q) \right), \tag{39}$$

decreases as N increases. In (39) $q_{\max}$ is the position of the peak maximum. The excess probability is calculated as the area between the curve $\langle \pi(q) \rangle_{S,N}$ and a curve obtained as a weighted sum of the limiting distribution (37) and the Gaussian peak (38), to the left of the maximum of the peak. The weights $(N-1)/N$ and $1/N$ correspond to the fractions of boxes occupied by the critical subsystem and the condensate, respectively.

For example, for the three graphs shown in Fig. 1(b), which correspond to $N = 2^k + 1$ with $k = 11, 12, 13$, the excess probability accumulated in the tail as compared to the probability $1/N$ accumulated in the peak, $P_{\rm dev}/(1/N)$, is approximately 4.2%, 2.8%, and 1.8%, respectively. To summarize, the analysis shows that there is a single peak in the particle distribution that detaches from the bulk. The area under this peak is approximately $1/N$, which means that the peak comes from a single box, where the condensate resides. The bulk part of the distribution approaches the critical distribution with deviations from the limiting shape being finite-size effects. This picture was rigorously proven in [8,30–36]. The

details of the approach to the thermodynamic limit determines the origin of the subleading corrections. As noted in the Introduction [4–11], the particle distribution can be regarded as being the nonequilibrium steady state of a zero-range process with suitably chosen rates. The relocation dynamics of the condensate at the critical density will then, with suitable scaling, be dominated by switching to a (distributed) metastable fluid [33–35]. On the other hand, if the density is fixed to be strictly larger than the critical density in taking the thermodynamic limit, the condensate will transfer via a subcondensate and distributed fluid configurations will eventually be much less likely than sharing the excess mass between just two sites [8,36]. The subcondensate is responsible for the shape of the deviations in the elongated left tails of the peaks. In this picture the subcondensate is a rare event whose probability tends to zero when the system size increases, as illustrated by the numerical analysis of $P_{\rm dev}$ above.

V. POWER-LAW WEIGHTS

Consider weights of the form

$$\tilde{w}(s) = s^{-\beta} e^{\lambda+\sigma s} \quad \text{for } s = 1, 2, \ldots, \tag{40}$$

with β, λ, and σ arbitrary real parameters. These weights can be reduced to power-law weights

$$w(s) = s^{-\beta} \quad \text{for } s = 1, 2, \ldots \tag{41}$$

by the transformation (5) $\tilde{w}(s) \to w(s) = e^{-\lambda-\sigma s}\tilde{w}(s)$. As follows from (6), the ensemble averages for the power-law weights (41) are the same as for the weights $\tilde{w}(s)$ (40). We will therefore restrict ourselves to the weights (41), which are representative for the whole family (40). The generating function $K(\alpha)$ is

$$K(\alpha) = \ln \mathrm{Li}_\beta(e^{-\alpha}), \tag{42}$$

where $\mathrm{Li}_\beta(z)$ is the polylogarithm [38]

$$\mathrm{Li}_\beta(z) = \sum_{k=1}^{\infty} \frac{z^k}{k^\beta}. \tag{43}$$

The asymptotic behavior of $K(\alpha)$ for $\alpha \to 0^+$ can be deduced from the asymptotic behavior of the polylogarithm, which is discussed in Appendix B. It depends on β. Regarding the critical behavior of the model we can distinguish four cases, which lead to different types of the free-energy density behavior.

(A) $K''(0) < \infty$ for $\beta \in (3, +\infty)$.
(B) $K''(0) = \infty$ but $K'(0) < \infty$ for $\beta \in (2, 3]$.
(C) $K'(0) = \infty$ but $K(0) < \infty$ for $\beta \in (1, 2]$.
(D) $K(0) = \infty$ for $\beta \in (-\infty, 1]$.

The free-energy density $\phi(r)$ (14) can be calculated using the saddle-point equations (24) and (25), which lead to a parametric representation of $\phi(r)$,

$$r = -\frac{1}{K'(\alpha)}, \quad \phi(r) = \alpha - \frac{K(\alpha)}{K'(\alpha)}, \tag{44}$$

with the parameter α which varies in the range $(0, \infty)$. These equations hold for $r > r_c$. The critical value is

$$r_c = -\frac{1}{K'(0)} = \frac{\zeta(\beta)}{\zeta(\beta-1)} \tag{45}$$

for cases A and B and $r_c = 0$ for C and D. For $0 < r \leqslant r_c$ the free-energy grows linearly with r,

$$\phi(r) = rK(0) = r \ln \zeta(\beta). \tag{46}$$

The behavior of $\phi(r)$ is illustrated in Fig. 2(a) for $\beta = 7/2, 5/2, 3/2, 1/2$, which are representative for the four cases. The curves are obtained by the parametric equations (44). The linear part of the solution (46), which corresponds to the condensed phase, is shown by the dashed line. The derivative $\phi'(r)$ is shown in Fig. 2(b). It is calculated from Eq. (24), which gives $\phi'(r) = K(\alpha(r))$. In combination with (25), this leads to the parametric equations for the derivative,

$$r = -\frac{1}{K'(\alpha)}, \quad \phi'(r) = K(\alpha), \tag{47}$$

for $r > r_c$, with the parameter α which varies in the range $(0, \infty)$. For $0 < r \leqslant r_c$ the derivative is constant,

$$\phi'(r) = K(0), \tag{48}$$

as follows from (44) and (46). For cases A and B the derivative $\phi'(r)$ is constant for $0 \leqslant r \leqslant r_c$. For $r \to 1$ the derivative $\phi'(r)$ tends to $-\infty$. For $r \to 0$ it tends to $K(0)$, which is finite for A–C and infinite for D. The main difference between cases A and B is that the second derivative $\phi''(r)$ is continuous at r_c for B and discontinuous for A. More precisely (see Appendix C), when the critical point is approached from the fluid phase side $r \to r_c^+$, the second derivative $\phi''(r)$ behaves at the critical point r_c as

$$\phi''(r) = \begin{cases} -c_1(r-r_c)^x + \cdots & \text{for } \beta \in (2, 3) \\ +c_2 \ln(r-r_c) + \cdots & \text{for } \beta = 3 \\ -c_3 + \cdots & \text{for } \beta \in (3, \infty), \end{cases} \tag{49}$$

where

$$x = \frac{3-\beta}{\beta-2} \tag{50}$$

is a positive exponent and c_1, c_2, c_3 are positive constants that depend on β. The ellipses indicate subleading terms. On the other hand, the second derivative is zero $\phi''(r) = 0$ in the condensed phase, that is, for $r < r_c$. This means that the phase transition is second order for $\beta \in (3, +\infty)$, with a finite discontinuity of $\phi''(r)$ at the critical value $r = r_c$. For $\beta = 3$, the phase transition is also second order but $\phi''(r)$ has a logarithmic discontinuity $\ln(r - r_c)$, as r approaches r_c from above. For $\beta \in (2, 3)$, the phase transition is of third or higher order. The order of the transition increases when β approaches 2 and the transition eventually disappears for $\beta = 2$. There is no phase transition for $\beta \leqslant 2$.

VI. GRAND-CANONICAL ENSEMBLE

So far we have considered a system of S particles in N boxes and analyzed its behavior in the thermodynamic limit (12) as a function of the limiting particle density $\rho = 1/r = S/N$. Now we will consider a system with a variable number of boxes N, which is controlled by "chemical potential" μ, which is equal to the energy that can be absorbed or released in the system due to a change of the number of boxes by one.

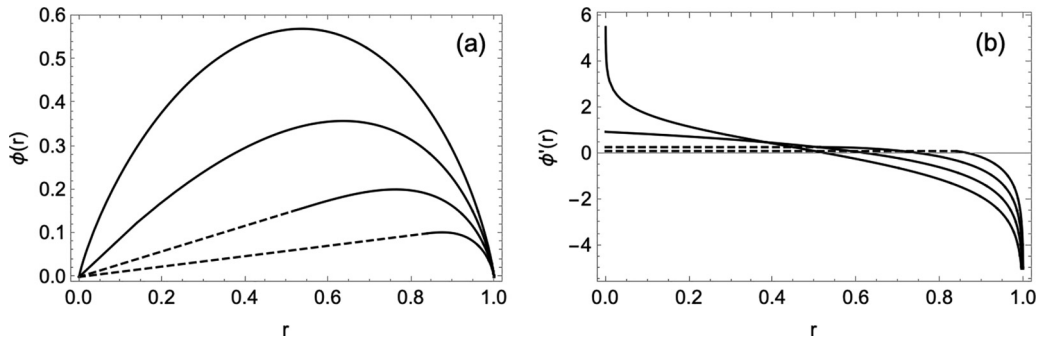

FIG. 2. (a) Free-energy density $\phi(r)$ and (b) its derivative $\phi'(r)$ for $\beta = 1/2$, $3/2$, $5/2$, and $7/2$ from top to bottom. There is a phase transition for $\beta = 7/2$ and $5/2$ at $r_c = \zeta(\beta)/\zeta(\beta-1)$ which is approximately at 0.8399 and 0.5135, respectively.

The corresponding partition function is [3,36]

$$Z_{S,\mu} = \sum_{N=1}^{S} e^{-\mu N} Z_{S,N}. \tag{51}$$

The system described by the partition function (51) will be a called grand-canonical ensemble.

The grand-canonical averages are defined as

$$\langle O\rangle_{S,\mu} = \frac{1}{Z_{S,\mu}} \sum_{N=1}^{S} e^{-\mu N} Z_{S,N} \langle O\rangle_{S,N}. \tag{52}$$

A general comment on notation is in order: We will distinguish between canonical averages and grand-canonical ones by the subscripts of the brackets, which will be S, N in the first case and S, μ in the second.

As before, let us discuss the particle distribution. The grand-canonical average is

$$\langle \pi(q)\rangle_{S,\mu} = \frac{w(q)}{Z_{S,\mu}} \sum_{N=1}^{S-q+1} e^{-\mu N} Z_{S-q,N-1}, \tag{53}$$

as directly follows from the definition (52). The contribution to the sum from $N = 1$ has to be treated carefully, because if there is only one box it must contain all particles. Therefore, for $N = 1$ the expression $Z_{S-q,N-1}$ on the right-hand side (53) should be interpreted as $Z_{S-q,0} = \delta_{S-q}$ [see Eq. (3)]. Taking this into account, we can rewrite (53) as

$$\langle \pi(q)\rangle_{S,\mu} = e^{-\mu} w(q) \frac{Z_{S-q,\mu}}{Z_{S,\mu}} + e^{-\mu} w(S) \frac{\delta_{S-q}}{Z_{S,\mu}} \tag{54}$$

for $q = 1, 2, \ldots, S$. We are now interested in the behavior of grand-canonical averages in the thermodynamic limit $S \to \infty$. To describe properties of the system in this limit, we define the thermodynamic potential

$$\psi(\mu) = \lim_{S\to\infty} \frac{1}{S} \ln Z_{S,\mu}. \tag{55}$$

Again, with a slight misuse of terminology, $\psi(\mu)$ can be called grand potential or the Landau free-energy density, in analogy to the free-energy density $\phi(r)$ (14), which was defined for the canonical ensemble. The two thermodynamic potentials are related to each other by the Legendre-Fenchel transform

$$\psi(\mu) = \sup_{r\in[0,1]} [-\mu r + \phi(r)]. \tag{56}$$

Indeed, approximating the grand-canonical partition function (51) by an integral and extracting its leading exponential behavior (23)

$$Z_{S,\mu} \propto e^{S\psi(\mu)} \propto \int_0^1 dr\, e^{S[-\mu r + \phi(r)]} \tag{57}$$

leads to (56). The inverse transform is

$$\phi(r) = \sup_{\mu\in R} [\mu r + \psi(\mu)]. \tag{58}$$

In most cases it reduces to

$$\phi(r) = \mu(r) r + \psi(\mu(r)), \tag{59}$$

with $\mu(r)$ a solution of

$$r = -\psi'(\mu). \tag{60}$$

Comparing (24) and (59), we find the consistency equations

$$\mu = K(\alpha), \tag{61}$$

$$\alpha = \psi(\mu), \tag{62}$$

from which we can deduce that the grand-canonical thermodynamic potential $\psi(\mu)$ (55) is the inverse function of the cumulant generating function (22) $\psi(\mu) = K^{-1}(\mu)$ or, equivalently, that

$$\psi(K(\alpha)) = \alpha, \quad K(\psi(\mu)) = \mu. \tag{63}$$

It follows that $K'(\psi(\mu)) = 1/\psi'(\mu)$, which shows that also Eqs. (25) and (60) are consistent. Using this exact relation, we can calculate the average $r = r(\mu)$ in the thermodynamic limit $S \to \infty$ in the grand-canonical ensemble

$$r(\mu) = \lim_{S\to\infty} \frac{\langle N\rangle_{S,\mu}}{S} = -\psi'(\mu) = \frac{-1}{K'(K^{-1}(\mu))}. \tag{64}$$

This result holds for $\mu \leqslant \mu_c$, where μ_c is the critical value of the chemical potential given by

$$\mu_c = K(\alpha_c), \tag{65}$$

where α_c is given by (27). For power-law weights (41) $\alpha_c = 0$. When the chemical potential exceeds the critical value $\mu > \mu_c$, the saddle-point equation breaks down and the average $r = r(\mu)$ (64) drops to zero. In this case N grows sublinearly with S for $S \to \infty$.

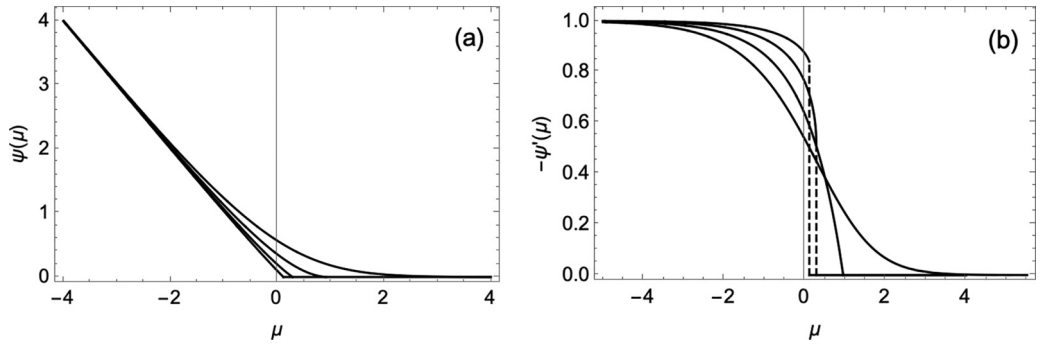

FIG. 3. (a) Landau free-energy density $\psi(\mu)$ and (b) its derivative $\psi'(\mu)$ for $\beta = 7/2, 5/2, 3/2$, and $1/2$ [from bottom to top in (a)]. The critical values $\mu_c = \ln \zeta(\beta)$ are approximately 0.1193, 0.2938, and 0.9603 for $\beta = 7/2, 5/2$, and $3/2$, respectively, and there is no transition for $\beta = 1/2$. Dashed straight lines in (b) indicate the discontinuities of size $r_c = \zeta(\beta)/\zeta(\beta - 1)$ in $\psi'(\mu)$ at μ_c, which are 0.8399 and 0.5135 for $\beta = 7/2$ and $5/2$, respectively.

The box-occupation probability in the fluid phase in the grand-canonical ensemble can be calculated in the thermodynamic limit as follows. For large S ($S \gg 1$) the partition function $Z_{S,\mu}$ (57) can be approximated by $e^{S\psi(\mu)}$ (57). Substituting this into (54), we get

$$\langle \pi(q) \rangle_{S,\mu} = w(q) e^{-q\psi(\mu)-\mu}. \tag{66}$$

Using the consistency relations (61) and (62), we see that the canonical and grand-canonical averages of the box-occupation probability (29) and (66) are identical

$$\langle \pi(q) \rangle_{S,\mu} = \langle \pi(q) \rangle_{S,N} \quad \text{for } S \to \infty \tag{67}$$

with the particle density in the canonical ensemble related to the chemical potential in the grand-canonical ensemble as $N/S = -K'(K^{-1}(\mu))$ (64). The equivalence holds in the saddle-point regime (fluid phase), that is, for $\mu < \mu_c$ (65). It breaks down at $\mu = \mu_c$. For $\mu > \mu_c$ the average number of boxes $\langle N \rangle_{S,\mu}$ approaches a constant independent of S for $S \to \infty$. Systems with a constant number of boxes and the number of particles tending to infinity exhibit a condensation of almost all particles in a single box [36].

To illustrate the different types of possible behavior of the Landau free-energy density $\psi(\mu)$, let us draw curves showing $\psi(\mu)$ and $\psi'(\mu)$ for power-law weights (41) for different β. As for the free-energy density (see Fig. 2), we will show in each plot curves for $\beta = 7/2, 5/2, 3/2$, and $1/2$. The curves will be generated as parametric plots. To plot $\psi(\mu)$ we use the fact that ψ is the inverse function of K (63), which is equivalent to the parametric equation

$$\mu = K(\alpha), \quad \psi(\mu) = \alpha, \tag{68}$$

with the parameter $\alpha > \alpha_c$, which for power-law weights (41) $\alpha_c = 0$. For $\psi'(\mu)$ we have the parametric equations

$$\mu = K(\alpha), \quad \psi'(\mu) = \frac{1}{K'(\alpha)}, \tag{69}$$

which are a direct consequence of ψ being the inverse function of K. The results are shown in Fig. 3. For power-law weights (41) the critical value of the chemical potential is

$$\mu_c = K(0) = \ln \zeta(\beta). \tag{70}$$

Note that the parametric equations for $\psi'(\mu)$ (69) are almost identical to those for $\phi'(r)$ (47). There are two differences. The first is that there is a minus sign in front of $1/K'(\alpha)$ in the equations for $\psi'(r)$ which is absent in the equations for $\psi'(\mu)$. The second is that the right-hand sides of these equations are swapped, which means that the ordinate and abscissa switch roles. This is not surprising because $\psi(r)$ and $\phi(\mu)$ are related to each other by the Legendre-Fenchel transformation. In other words, the drawings of $\psi'(\mu)$ and $\phi'(r)$ (compare Figs. 3 and 2) can be obtained from each another by swapping the vertical and horizontal axes and changing the direction of the vertical axis.

So far we have discussed the case of power-law weights (41). The question is what the corresponding plots look like for the family of weights (40). Again, this can answered using the transformation $w(s) \to e^{\lambda+\sigma s} w(s)$ (5). Under this transformation, the free-energy density (14) transforms as

$$\phi(r) \to \phi(r) + \sigma + r\lambda \tag{71}$$

and the grand potential transforms as

$$\psi(\mu) \to \psi(\mu - r) + \sigma, \tag{72}$$

as follows from (56). The derivatives transform as

$$\phi'(r) \to \phi'(r) + \lambda \tag{73}$$

and

$$\psi'(\mu) \to \psi'(\mu - \lambda), \tag{74}$$

respectively. This means that the curve $\phi'(r)$ (see Fig. 2) moves up by λ and the curve $\psi'(\mu)$ (see Fig. 3) moves right by λ when power-law weights (41) are changed to (40). The critical value r_c (28) does not change. The critical value μ_c (70) is shifted by λ from $\ln \zeta(\beta)$ to

$$\mu_c = \ln \zeta(\beta) + \lambda. \tag{75}$$

The parameter σ has no effect on the critical values r_c and μ_c.

Returning to purely power-law weights, let us now concentrate on the phase transition, i.e., on the behavior of the grand potential $\psi(\mu)$ near the critical point μ_c (70). A detailed analysis is presented in Appendix D. For $\mu \to \mu_c^-$ the grand

potential behaves as

$$\psi'(\mu) = \begin{cases} -C(\mu_c - \mu)^y + \cdots & \text{for } \beta \in (1,2) \\ \zeta(2)/\ln(\mu_c - \mu) + \cdots & \text{for } \beta = 2 \\ -r_c + \cdots & \text{for } \beta \in (2, +\infty), \end{cases} \tag{76}$$

where

$$y = \frac{2-\beta}{\beta - 1} \tag{77}$$

is a positive exponent and C is a positive constant depending on β. The ellipses indicate subleading terms. On the other hand, $\psi'(\mu) = 0$ for $\mu > \mu_c$. This means that the phase transition is first order for $\beta \in (2, +\infty)$. For $\beta \in (1, 2]$ the order of the phase transition varies from second to infinite. More precisely, the interval $\beta \in (1, 2]$ can be divided into subintervals $\beta \in (1 + 1/n, 1 + 1/(n-1)]$, $n = 2, 3, \ldots$, in which the nth derivative is discontinuous. The transition disappears for $\beta = 1$.

VII. OTHER ENSEMBLES

One can consider a system with N boxes and a variable number of particles. The partition function

$$Z_{\alpha,N} = \sum_{S=N}^{\infty} e^{-\alpha S} Z_{S,N} \tag{78}$$

describes the possible states of such a system in equilibrium with a common reservoir that each box is in contact with. In the thermodynamic limit the reservoir is assumed to contain infinitely many particles. The fugacity α plays the role of the chemical potential of a particle. It is easy to see that the partition function factorizes in this case

$$Z_{\alpha,N} = e^{NK(\alpha)}, \tag{79}$$

so it describes N independent boxes, each contributing energy $-K(\alpha)$ to the total energy of the system. The contributions from different boxes are thus entirely independent and the partition function factorizes into the product of single-urn or -box partition functions [39,40]. The average particle density is $\rho(\alpha) = -K'(\alpha)$. For power-law weights (41) with $\beta \leqslant 1$, the density $\rho(\alpha)$ becomes infinite for $\alpha \leqslant 0$. For $\beta > 1$, the density $\rho(\alpha)$ becomes infinite for $\alpha < 0$. This infinite density means that each box absorbs infinitely many particles from the reservoir.

In principle, also an ensemble with varying numbers of particles and boxes can be defined by the partition function

$$Z_{\alpha,\mu} = \sum_{N=1}^{\infty} e^{-\mu N} Z_{\alpha,N} = \sum_{N=1}^{\infty} e^{[-\mu + K(\alpha)]N}, \tag{80}$$

which is convergent for $\mu > K(\alpha)$ and $\alpha > \alpha_c$, yielding

$$Z_{\alpha,\mu} = \frac{1}{e^{\mu - K(\alpha)} - 1}. \tag{81}$$

This expression becomes infinite for $\mu \to K(\alpha)$; the sum (80) diverges. From this partition function one can also calculate the grand-canonical partition function $Z_{S,\mu}$ (51),

$$\frac{1}{e^{\mu - K(\alpha)} - 1} = \sum_{S=1}^{\infty} e^{-\alpha S} Z_{S,\mu}. \tag{82}$$

as an inverse Laplace transform.

VIII. PROBABILISTIC AND QUASIPROBABILISTIC NORMALIZATION OF WEIGHTS

In some problems it is convenient to normalize the weights $w(s)$ in the partition function (1),

$$\hat{w}(s) = \frac{w(s)}{\sum_{q=1}^{\infty} w(q)}, \tag{83}$$

so that the model after the normalization can be interpreted in a probabilistic manner. This can be done only if the sum in the denominator on the right-hand side in (83) is finite. The normalization can be obtained by the transformation (5) with $\sigma = 0$ and $\lambda = -\ln[\sum_{q=1}^{\infty} w(q)]$ and therefore it has no effect on the statistical averages (6).

There are however families of weights which cannot be normalized because the normalization sum in (83) is infinite. For example, the constant weights $w(s) = 1$ for $s = 1, 2, \ldots$ cannot be normalized. As a way around this problem, some authors have proposed a quasiprobabilistic normalization [20] by putting an upper limit on the weights (and hence sum)

$$\hat{w}(s, S) = \frac{w(s)}{\sum_{s=1}^{S} w(s)} = \frac{w(s)}{\Omega(S)} \tag{84}$$

for $s = 1, 2, \ldots, S$ and $\hat{w}(s, S) = 0$ for $s > S$. The normalization constant $\Omega(S)$ depends on S. It is finite for any finite S. For example, $\Omega(S) = S$ for the trivial weights $w(s) = 1$. This type of cut-off grand-canonical ensemble has also been introduced as a way to control finite-size effects for the urn model with weights that lead to a slow convergence to the thermodynamic limit [32].

The model with the quasiprobabilistic normalization can be obtained from the original weights by the transformation (5) with $\lambda = -\ln \Omega(S)$. This leads to the relationship between the partition functions

$$\hat{Z}_{S,N} = e^{-N\Omega(S)} Z_{S,N} \tag{85}$$

and

$$\hat{Z}_{S,\mu} = Z_{S,\mu + \ln \Omega(S)}, \tag{86}$$

where the partition functions on the right-hand side of the equations above are defined by weights independent of S [see Eqs. (1) and (51)].

We note that the model with the quasiprobabilistic normalization (84) is no longer invariant with respect to the transformation (5), because $\Omega(S)$ changes under this transformation. It therefore makes a difference whether one considers purely power-law weights $q^{-\beta}/\Omega(S)$ or exponentially damped ones $q^{-\beta} e^{-\sigma q}/\Omega(S)$. We stress that the weights $w(s)$ in the partition functions (1) and (51) depend only on the occupation of the box, while in the quasiprobabilistic model the weights $\hat{w}(s, S)$ depend also on S. The quasiprobabilistic model therefore belongs to a different class.

In the rest of this section we will consider the quasiprobabilistic model with the power-law weights (41) in the grand-canonical ensemble for $\mu = 0$, which corresponds to the model discussed in the main part of this paper (51) with a running chemical potential

$$\mu(S) = \ln \Omega(S) = \ln \sum_{s=1}^{S} s^{-\beta}. \tag{87}$$

This follows from (86). For $\beta > 1$, the running chemical potential $\mu(S)$ approaches the critical value $\mu_c = \ln \zeta(\beta)$ from below $\mu(S) \to \mu_c^-$ when S increases. The difference $\mu_c - \mu(S)$ behaves as

$$\mu_c - \mu(S) = \ln\left(1 - \frac{\zeta(\beta, S+1)}{\zeta(\beta)}\right), \tag{88}$$

where $\zeta(\beta, S)$ is the Hurwitz zeta function [38]. The difference tends to zero as

$$\mu_c - \mu(S) = \frac{1}{(\beta-1)\zeta(\beta)} S^{-(\beta-1)} + \cdots \tag{89}$$

for $S \to \infty$. The ellipsis indicates subleading terms. We can compute the average inverse density at $\mu(S)$ using the equation (64) for $S \gg 1$,

$$r(S) = \frac{\langle N \rangle_{S,\mu(S)}}{S} = -\psi'(\mu(S)). \tag{90}$$

For $\beta \in (2, \infty)$, $r(S)$ tends to the critical value $\zeta(\beta)/\zeta(\beta-1)$ for $S \to \infty$. For $\beta \in (1, 2)$, $r(S)$ behaves asymptotically as $r(S) \sim S^{\beta-2}$ for large S, as can be seen by substituting (89) into (D10). For $\beta \in (-\infty, 1]$ there is no phase transition. In this case $\mu(S)$ (87) grows asymptotically as $\mu(S) \sim (-\beta+1)\ln(S)$. Substituting this into (D13), we see that $r(S)$ behaves asymptotically as $r(S) \sim 1/S$ for large S. These results translate into (90)

$$\langle N \rangle_{S,\mu(S)} = \begin{cases} c_1 S + \cdots & \text{for } \beta \in (2, \infty) \\ c_2 S^{\beta-1} + \cdots & \text{for } \beta \in (1, 2) \\ c_3 + \cdots & \text{for } \beta \in (-\infty, 1) \end{cases} \tag{91}$$

for $S \to \infty$, with some positive coefficients c_1, c_2, and c_3 depending on β, where the ellipses again indicate subleading terms. The detailed results, also for the borderline cases of $\beta = 1$ and 2, can be found in [20].

Let us stress that the model with weights normalized by the pseudoprobabilistic condition (84) corresponds to the model discussed in the main part of this paper (51) with a running chemical potential $\mu = \ln \Omega(S)$ (87). For $\beta > 1$, the effective chemical potential $\mu = \ln \Omega(S)$ approaches the critical value $\mu_c = \ln \zeta(\beta)$ from below as S increases. For $\beta \leqslant 1$, the effective chemical potential tends logarithmically to infinity for $S \to \infty$. In both cases the system stays in the fluid phase, as long as S is finite. The effective particle probability distribution (66) for the system with the effective chemical potential $\mu = \ln \Omega(S)$ is

$$\langle \pi(q) \rangle_{S,\ln \Omega(S)} = \frac{w(q)}{\Omega(S)} e^{-q\psi[\ln \Omega(S)]}. \tag{92}$$

We thus see that the quasiprobabilistic normalization introduces weak exponential damping for large q into the effective particle distribution. The damping factor decays with S but disappears completely only in the limit $S \to \infty$.

IX. SUMMARY

After some general discussion of the urn model, we focused in this paper on the zeta-urn model, which is analytically solvable. We used this to determine the thermodynamic potentials that control the exponential growth of the canonical and grand-canonical partition functions in the thermodynamic limit and elucidate the critical behavior.

The second derivative of the free-energy density with respect to the particle density describes density fluctuations in the canonical ensemble. For $\beta > 3$ the second derivative is discontinuous at the critical point, so the transition is of the second order. For $\beta = 3$ the second derivative has a logarithmic divergence. For $\beta \in (2, 3]$ the order of the transition changes at the discrete values $\beta_n = 2 + 1/(n-1)$, $n = 2, 3, \ldots$, where n is the order of the transition for $\beta \in (\beta_{n+1}, \beta_n]$. There is no phase transition for $\beta \leqslant 2$.

For the grand-canonical ensemble the situation is different. The first derivative of the corresponding thermodynamic potential is discontinuous for $\beta > 2$, so the phase transition is of the first order in this case. For $\beta \in (1, 2]$ the order of the transition changes at the discrete values $\beta'_n = 1 + 1/(n-1)$, where $n = 2, 3, \ldots$ is the order of the transition for $\beta \in (\beta'_{n+1}, \beta'_n]$. There is no phase transition for $\beta \leqslant 1$.

The thermodynamic potentials for the canonical and grand-canonical ensembles can be derived from each other. More specifically, the function $\phi'(r)$ on the support $r \in (r_c, 1)$ is the inverse function of $\mu \to -\psi'(\mu)$ on the support $\mu \in (-\infty, \mu_c)$, which is a consequence of the Legendre-Fenchel transform, which relates the two functions. Additionally, we showed that the grand-canonical potential $\psi(\mu)$ on the support $\mu \in (-\infty, \mu_c)$ is the inverse function of the cumulant generating function $K(\alpha)$ on the support $\alpha \in (\alpha_c, \infty)$. The relation of other ensembles to the canonical and grand-canonical ensembles discussed in detail here was also explored, in particular those with probabilistic and quasiprobabilistic weights which can be useful both for normalizing otherwise divergent sums and for controlling finite-size effects.

It is perhaps worth emphasizing that the zeta-urn model provides a useful toy model for investigating phase transitions of any order, including discontinuous ones in the case of the grand-canonical ensemble, by the simple expedient of varying a single parameter, the exponent β in the power-law weights. The finite-size partition functions are, at least in principle, exactly calculable and can be compared with the asymptotic results of saddle-point expansions to explore the finite-size effects at the transition with β tuned to give the desired order.

In the following paper [41] we use some of the results presented in this paper to study the Rényi entropy and diversity measures [20,42] for the zeta-urn model and discuss their singular behavior and other properties in the thermodynamic limit (12) in the canonical ensemble. In contrast, the grand-canonical ensemble is employed in [43] to investigate the behavior of the partition function zeros of the zeta urn as β is varied and the order of the transition changes.

ACKNOWLEDGMENT

The authors would like to thank Paul Chleboun for a helpful discussion on finite-size corrections.

APPENDIX A: DERIVATION OF THE PARTICLE DISTRIBUTION IN THE THERMODYNAMIC LIMIT

The starting point of the calculation is Eq. (8). We replace the partition functions in the numerator and denominator on the right-hand side of this equation by their asymptotic forms, which follow the saddle-point approximation (23),

$$Z_{S,N} \propto e^{S\alpha(r)+NK(\alpha(r))} \tag{A1}$$

and

$$Z_{S-q,N-1} \propto e^{(S-q)\alpha(\tilde{r})+(N-1)K(\alpha(\tilde{r}))}, \tag{A2}$$

where $r = N/S$ and $\tilde{r} = (N-1)/(S-q)$. In the limit (12) $\tilde{r}$ can be expanded in $1/S$:

$$\tilde{r} = r + \frac{qr-1}{S} + o\left(\frac{1}{S}\right). \tag{A3}$$

It follows that

$$\alpha(\tilde{r}) = \alpha(r) + \alpha'(r)\frac{qr-1}{S} + o\left(\frac{1}{S}\right) \tag{A4}$$

and

$$K(\alpha(\tilde{r})) = K(\alpha(r)) + K'(\alpha(r))\alpha'(r)\frac{qr-1}{S} + o\left(\frac{1}{S}\right). \tag{A5}$$

Using the saddle-point equation (25), we can replace $K'(\alpha(r))$ in (A5) with $-1/r$:

$$K(\alpha(\tilde{r})) = K(\alpha(r)) - \alpha'(r)\frac{qr-1}{rS} + o\left(\frac{1}{S}\right). \tag{A6}$$

Inserting these expansions into (A2), we get

$$\begin{aligned} Z_{S-q,N-1} \propto \exp[&(S-q)\alpha(r) + (N-1)K(\alpha(r)) \\ &+ \alpha'(r)(qr-1)^2/rS + o(S^{-1})]; \end{aligned} \tag{A7}$$

hence

$$\begin{aligned} \frac{Z_{S-q,N-1}}{Z_{S,N}} \propto \exp[&-q\alpha(r) - K(\alpha(r)) \\ &+ \alpha'(r)(qr-1)^2/rS + o(s^{-1})] \end{aligned} \tag{A8}$$

and finally (8)

$$\langle \pi(q) \rangle_{S,N} \propto w(q)\exp[-q\alpha(r) - K(\alpha(r)) + O(S^{-1})]. \tag{A9}$$

APPENDIX B: ASYMPTOTICS OF THE POLYLOGARITHM

For noninteger β, the polylogarithm of $e^{-\alpha}$ has the following series expansion at $\alpha_c = 0$:

$$\mathrm{Li}_\beta(e^{-\alpha}) = \Gamma(1-\beta)\alpha^{\beta-1} + \sum_{k=0}^{\infty} \frac{(-1)^k \zeta(\beta-k)}{k!}\alpha^k. \tag{B1}$$

For integer β, the singular term contains a logarithmic singularity

$$\begin{aligned} \mathrm{Li}_\beta(e^{-\alpha}) = &\frac{(-1)^{\beta-1}}{(\beta-1)!}[H_{\beta-1} - \ln(\alpha)]\alpha^{\beta-1} \\ &+ \sum_{k=0,k\neq\beta-1}^{\infty} \frac{(-1)^k \zeta(\beta-k)}{k!}\alpha^k, \end{aligned} \tag{B2}$$

where $H_n = 1 + 1/2 + \cdots + 1/n$ is the nth harmonic number.

APPENDIX C: SINGULARITIES OF THE (CANONICAL) FREE-ENERGY DENSITY AT THE CRITICAL POINT

In this Appendix we will discuss singularities of the free-energy density $\phi(r)$ at the critical point $r = r_c$. This is the point where the solid line changes to the dashed line for $\beta = 5/2, 7/2$ in Fig. 2. The analysis will be performed on the basis of parametric equations (44), which allow us to extract the singularity of the free-energy density. The main components of these equations are the function $K(\alpha)$ and its derivative $K'(\alpha)$, so to prepare the ground let us analyze the behavior of these functions for α close to $\alpha_c = 0$, which correspond to r close to r_c.

For cases D and C, that is, for $\beta \in (-\infty, 2]$, there is no phase transition as $r_c = 0$. So we will concentrate on the range $\beta \in (2, \infty)$. For noninteger we can write

$$K(\alpha) = \mu_c - \sum_{k=1}^{\lfloor\beta-1\rfloor} a_k\alpha^k - A\alpha^{\beta-1} + o(\alpha^{\beta-1}) \tag{C1}$$

and

$$-\frac{1}{K'(\alpha)} = r_c + \sum_{k=1}^{\lfloor\beta-2\rfloor} b_k\alpha^k + B\alpha^{\beta-2} + o(\alpha^{\beta-2}), \tag{C2}$$

where the symbol $\lfloor x \rfloor$ is the largest integer less than or equal to x. The constants μ_c and r_c on the right-hand side of these equations stand for $\mu_c = K(0)$ and $r_c = -1/K'(0)$, respectively. The coefficients a_k and b_k as well as A and B can be directly deduced from the expansion of $K(\alpha)$ (42). They depend on β, but the form of this dependence is inessential for further analysis. The signs of the coefficients are chosen for convenience. Only terms up to $\alpha^{\beta-1}$ in the (C1) and up to $\alpha^{\beta-2}$ in (C2) are displayed. All others are included in the little-o notation for $\alpha \to 0$.

We will separately consider the ranges $\beta \in (2, 3)$ and $\beta \in (3, +\infty)$, and the borderline case $\beta = 3$. We begin with $\beta \in (2, 3)$. The parametric equations (47) for the derivative $\phi'(r)$ become

$$\phi'(r) = \mu_c - a_1\alpha + o(\alpha) \tag{C3}$$

with

$$r = r_c + B\alpha^{\beta-2} + o(\alpha^{\beta-2}) \tag{C4}$$

for α close to $\alpha_c = 0$, as follows from (C1) and (C2). From (C4) we find that $\alpha = [(r-r_c)/B]^{1/(\beta-2)} + \cdots$ when r tends to r_c from above. Plugging this into (C3), we get

$$\phi'(r) - \mu_c = -C(r-r_c)^{1/(\beta-2)} + o((r-r_c)^{1/(\beta-2)}), \tag{C5}$$

where $C = a_1/B^{1/(\beta-2)}$. The second derivative behaves as

$$\phi''(r) \sim (r - r_c)^{(3-\beta)/(\beta-2)} \tag{C6}$$

for $r \to r_c^+$. The power $(3-\beta)/(\beta-2)$ is positive for $\beta \in (2.3)$, so this means that $\phi''(r_c^+) = 0$. Also, for $r \to r_c^-$ the second derivative is equal to zero, $\phi''(r_c^-) = 0$; hence the second derivative is continuous for $\beta \in (2, 3)$. In the same way it can be checked that the third derivative is continuous for $\beta \in (2, 5/2)$ and it is discontinuous for $\beta \in [5/2, 3)$. The transition is thus third order for $\beta \in [5/2, 3)$. More generally, the nth derivative $\phi^{(n)}(r)$ is discontinuous at r_c for $\beta \in [2 + 1/(n-1), 3)$. Therefore, the transition is of nth order for $\beta \in [2 + 1/(n-1), 2 + 1/(n-2))$ for $n = 3, 4, \ldots$. The order of the transition increases to infinity when β approaches 2. Eventually, at $\beta = 2$, the transition disappears completely.

Now consider the range $\beta \in (3, +\infty)$. We first focus on $\beta \in (3, 4)$. In this case Eq. (C4) takes the form

$$r = r_c + b_1\alpha + B\alpha^{\beta-2} + o(\alpha^{\beta-2}). \tag{C7}$$

For r close to r_c this gives

$$\alpha = \frac{r - r_c}{b_1} - \frac{B}{b_1}\left(\frac{r - r_c}{b_1}\right)^{\beta-2} + o((r - r_c)^{\beta-2}). \tag{C8}$$

Substituting this into (C3), we get

$$\phi'(r) - \mu_c = -\frac{a_1}{b_1}(r - r_c) + \frac{a_1 B}{b_1}\left(\frac{r - r_c}{b_1}\right)^{\beta-2} + o((r - r_c)^{\beta-2}). \tag{C9}$$

We see that the second derivative is discontinuous at r_c, because

$$\lim_{r \to r_c^+} \phi''(r) = -\frac{a_1}{b_1} \tag{C10}$$

and

$$\lim_{r \to r_c^-} \phi''(r) = 0, \tag{C11}$$

and the transition is therefore second order. We note in passing that the third derivative has an infinite discontinuity for $\beta \in (3, 4)$, coming from the term $(r - r_c)^{\beta-2}$ in (C9). The calculations can be repeated for $\beta \in (n, n+1]$, for $n = 3, 4, \ldots$, to see that in all these intervals the second derivative has a finite discontinuity and the derivative $\phi^{(n)}(r)$ has an infinite discontinuity at r_c.

Now consider the borderline case $\beta = 3$. The parametric equations (47) can be written as

$$\phi'(r) = \mu_c - a_1\alpha + o(\alpha) \tag{C12}$$

and

$$r = r_c + b_1\alpha + B\alpha \ln\alpha + o(\alpha \ln\alpha), \tag{C13}$$

as follows from (B2). Inverting (C13) for α, we find

$$\alpha = c_1(r - r_c) + C(r - r_c)\ln(r - r_c) + o((r - r_c)\ln(r - r_c)), \tag{C14}$$

where $c_1 = 1/b_1 + B/b_1^2 \ln b_1$ and $C = -B/b_1^2$. Substituting this into (C12), we get

$$\phi'(r) - \mu_c = -a_1c_1(r - r_c) - a_1C(r - r_c)\ln(r - r_c) + o((r - r_c)\ln(r - r_c)). \tag{C15}$$

Taking the derivative of both sides, we find that the second derivative has a logarithmic singularity for $r \to r_c^+$,

$$\phi''(r) = -a_1(c_1 + C) - a_1C\ln(r - r_c) + o(\ln(r - r_c)). \tag{C16}$$

APPENDIX D: SINGULARITIES OF THE GRAND POTENTIAL AT THE CRITICAL POINT

In this Appendix will determine the singularities of the grand potential $\psi(\mu)$ for the power-law weights (41) at the critical chemical potential $\mu_c = \ln\zeta(\beta)$ for $\beta > 1$. There is no phase transition for $\beta \leqslant 1$.

The initial point of the analysis is the parametric representation (69). The critical behavior is reproduced in the limit $\alpha \to 0^+$, which corresponds to $\mu_c - \mu \to 0^+$. We separately consider three cases: $\beta \in (2, \infty)$, $\beta = 2$, and $\beta \in (1, 2)$.

For $\beta \in (2, +\infty)$ we can use Eqs. (C1) and (C2) to cast the parametric equations (69) in the form

$$\psi'(\mu) = -r_c - \sum_{k=1}^{\lfloor\beta-2\rfloor} b_k\alpha^k - B\alpha^{\beta-2} + o(\alpha^{\beta-2}) \tag{D1}$$

and

$$\mu = \mu_c - a_1\alpha + o(\alpha). \tag{D2}$$

From (D2) we can calculate $\alpha = (\mu_c - \mu)/a_1 + o(\mu_c - \mu)$ for $\mu \to \mu_c^-$. Substituting this into (D1), we see that

$$\lim_{\mu \to \mu_c^-} \psi'(\mu) = -r_c, \tag{D3}$$

which is a negative number. On the other hand,

$$\lim_{\mu \to \mu_c^+} \psi'(\mu) = 0, \tag{D4}$$

so the first derivative has a discontinuity at $\mu = \mu_c$ and so the phase transition is of the first order. In addition, the first derivative has a power-law singularity $(\mu_c - \mu)^{\beta-2}$ [or $(\mu_c - \mu)^{\beta-2}\ln(\mu_c - \mu)$ for integer β] for $\mu \to \mu_c^-$. This singularity makes the nth and higher derivatives infinite for $\mu \to \mu_c^-$, where $n = \lfloor\beta\rfloor$.

For $\beta = 2$ there is no discontinuity of the first derivative. In this case the first derivative behaves as

$$\psi'(\mu) \sim \frac{\zeta(2)}{\ln[\zeta(2)(\mu_c - \mu)]} \tag{D5}$$

as μ approaches μ_c, so it vanishes in the limit $\mu \to \mu_c^-$. Taking the derivative of both sides, we see that the second derivative diverges as $\psi''(\mu) \sim (\mu_c - \mu)^{-1}[\ln(\mu_c - \mu)]^{-2}$ as μ tends to μ_c, so the transition is of the second order for $\beta = 2$.

For $\beta \in (1, 2)$ the expressions (C1) and (C2) reduce to

$$K(\alpha) = \mu_c - A\alpha^{\beta-1} + o(\alpha^{\beta-1}) \tag{D6}$$

and

$$-\frac{1}{K'(\alpha)} = B\alpha^{2-\beta} + o(\alpha^{\beta-2}). \tag{D7}$$

Therefore, for $\beta \in (1, 2)$ the parametric equations (69) take the form

$$\psi'(\mu) = -B\alpha^{2-\beta} + o(\alpha^{2-\beta}) \tag{D8}$$

and

$$\mu_c - \mu = A\alpha^{\beta-1} + o(\alpha^{\beta-1}) \tag{D9}$$

for $\alpha \to 0^+$. Extracting α from (D9) and substituting it into (D8) leads to [3]

$$\psi'(\mu) = -C(\mu_c - \mu)^{(2-\beta)/(\beta-1)} + o((\mu_c - \mu)^{(2-\beta)/(\beta-1)}), \tag{D10}$$

where $C = B/A^{1/(\beta-1)}$. The transition is of the second order for $\beta \in (3/2, 2]$, of the third order for $\beta \in (3/4, 3/2]$, and of the nth order for $\beta \in (1 + 1/n, 1 + 1/(n-1)]$. The transition softens when β approaches 1 and it eventually disappears for $\beta = 1$.

There is no phase transition for $\beta \in (-\infty, 1]$. This can be seen directly from the expansions of $K(\alpha)$ and $K'(\alpha)$, which in this range β instead of (C1) and (C2) take the form

$$K(\alpha) = \ln[\Gamma(1-\beta)] + (\beta - 1)\ln\alpha + o(\ln\alpha) \tag{D11}$$

and

$$-\frac{1}{K'(\alpha)} = \frac{\alpha}{1-\beta} + o(\alpha). \tag{D12}$$

From (D11) we see that $\mu = K(\alpha) \to \infty$ when $\alpha \to 0^+$. In other words, the critical point escapes to infinity. Extracting α from (D11) and substituting it into (D12), we see that $\psi'(\mu)$ (69) falls off exponentially for $\mu \to +\infty$,

$$\psi'(\mu) = -\frac{[\Gamma(1-\beta)]^{1/(1-\beta)}}{1-\beta} e^{-\mu/(1-\beta)} + o(e^{-\mu/(1-\beta)}). \tag{D13}$$

In particular, for $\beta = 0$, we see that $\psi'(\mu)$ falls off exponentially for $\mu \to \infty$ as $\psi'(\mu) \approx -e^{-\mu}$. This is consistent with the exact solution for $\beta = 0$. For $\beta = 0$ the grand-canonical partition function (51) can be calculated to give $Z_{S,\mu} = e^{-\mu}(1 + e^{-\mu})^{S-1}$ from $Z_{S,N}$ (10). In the thermodynamic limit we therefore find $\psi(\mu) = -\ln(1 + e^{-\mu})$ and $\psi'(\mu) = -e^{-\mu}/(1 + e^{-\mu}) \approx -e^{-\mu}$.

[1] P. Bialas, Z. Burda, and D. Johnston, Nucl. Phys. B **493**, 505 (1997).
[2] J. M. Drouffe, C. Godréche, and F. Camia, J. Phys. A: Math. Gen. **31**, L19 (1998).
[3] P. Bialas, Z. Burda, and D. Johnston, Nucl. Phys. B **542**, 413 (1999).
[4] F. Spitzer, Adv. Math. **5**, 246 (1970).
[5] M. R. Evans, Braz. J. Phys. **30**, 42 (2000).
[6] I. Jeon, P. March, and B. Pittel, Ann. Probab. **28**, 1162 (2000).
[7] M. R. Evans and T. Hanney, J. Phys. A: Math. Gen. **38**, R195 (2005).
[8] C. Godréche and J. M. Luck, J. Phys. A: Math. Gen. **38**, 7215 (2005).
[9] J. Kaupuzs, R. Mahnke, and R. J. Harris, Phys. Rev. E **72**, 056125 (2005).
[10] C. Godréche, Lect. Notes Phys. **716**, 261 (2007).
[11] B. Waclaw, L. Bogacz, Z. Burda, and W. Janke, Phys. Rev. E **76**, 046114 (2007).
[12] S. N. Majumdar, M. R. Evans, and R. K. P. Zia, Phys. Rev. Lett. **94**, 180601 (2005).
[13] M. R. Evans, S. N. Majumdar, and R. K. P. Zia, J. Stat. Phys. **123**, 357 (2006).
[14] M. R. Evans, S. N. Majumdar, and R. K. P. Zia, J. Phys. A: Math. Gen. **39**, 4859 (2006).
[15] P. Bialas and Z. Burda, Phys. Lett. B **384**, 75 (1996).
[16] S. Janson, Prob. Surveys **9**, 103 (2012).
[17] P. Bialas and Z. Burda, Phys. Lett. B **416**, 281 (1998).
[18] L. Bogacz, Z. Burda, and B. Waclaw, Phys. Rev. D **86**, 104015 (2012).
[19] Z. Burda, D. Johnston, J. Jurkiewicz, M. Kamiński, M. A. Nowak, G. Papp, and I. Zahed, Phys. Rev. E **65**, 026102 (2002).
[20] O. Mazzarisi, A. de Azevedo-Lopes, J. J. Arenzon, and F. Corberi, Phys. Rev. Lett. **127**, 128301 (2021).
[21] Y. Kafri, E. Levine, D. Mukamel, G. M. Schütz, and J. Török, Phys. Rev. Lett. **89**, 035702 (2002).
[22] M. R. Evans, E. Levine, P. K. Mohanty, and D. Mukamel, Eur. Phys. J. B **41**, 223 (2004).
[23] A. G. Angel, T. Hanney, and M. R. Evans, Phys. Rev. E **73**, 016105 (2006).
[24] P. Bialas, Z. Burda, and B. Waclaw, AIP Conf. Proc. **776**, 14 (2005).
[25] L. Van Hove, Phys. Rev. **89**, 1189 (1953).
[26] J. G. Wendel, Math. Scand. **14**, 21 (1964).
[27] C. Godréche, J. Phys. A: Math. Theor. **50**, 195003 (2017).
[28] C. Godréche, J. Phys. A: Math. Theor. **54**, 038001 (2021).
[29] D. Denisov, A. B. Dieker, and V. Shneer, Ann. Probab. **36**, 1946 (2008).
[30] S. Grosskinsky, G. M. Schütz, and H. Spohn, J. Stat. Phys. **113**, 389 (2003).
[31] P. A. Ferrari, C. Landim, and V. V. Sisko, J. Stat. Phys. **128**, 1153 (2007).
[32] P. Chleboun and S. Grosskinsky, J. Stat. Phys. **140**, 846 (2010).
[33] I. Armendariz, S. Grosskinsky, and M. Loulakis, Stoch. Proc. Appl. **123**, 3466 (2013).
[34] P. Chleboun and S. Grosskinsky, J. Stat. Phys. **154**, 432 (2014).
[35] W. Jatuviriyapornchai, P. Chleboun, and S. Grosskinsky, J. Stat. Phys. **178**, 682 (2020).
[36] C. Godréche, J. Stat. Phys. **182**, 13 (2021).
[37] B. V. Gnedenko and A. N. Kolmogorov, *Limit Distributions for Sums of Independent Random Variables* (Addison-Wesley, Cambridge, 1968).

[38] M. Abramowitz and I. A. Stegun, *Handbook of Mathematical Functions with Formulas, Graphs, and Mathematical Tables* (Dover, New York, 1972).
[39] B. Gaveau and L. Schulman, J. Phys. A: Math. Gen. **20**, 2865 (1987).
[40] G. Roepstor and L. Schulman, J. Stat. Phys. **34**, 35 (1984).
[41] P. Bialas, Z. Burda, and D. Johnston, following paper, Phys. Rev. E **108**, 064108 (2023).
[42] A. J. Wood, R. A. Blythe, and M. R. Evans, J. Phys. A: Math. Theor. **50**, 475005 (2017).
[43] P. Bialas, Z. Burda, and D. Johnston, Con. Matt. Phys., https://www.icmp.lviv.ua/journal/index.html.